

# Coexistence of $p$ -wave Magnetism and Superconductivity

Pavlo Sukhachov,<sup>1</sup> Hans Glöckner Giil,<sup>1</sup> Bjørnulf Brekke,<sup>1</sup> and Jacob Linder<sup>1</sup>

<sup>1</sup>Center for Quantum Spintronics, Department of Physics, Norwegian University of Science and Technology, NO-7491 Trondheim, Norway

(Dated: December 18, 2024)

The symmetry requirements for realizing unconventional compensated magnets with spin-polarized bands such as altermagnets have recently been uncovered. The most recent addition to this family of magnets is parity-odd or  $p$ -wave magnets. We demonstrate that  $p$ -wave magnets are perfectly compatible with superconductivity due to the spin polarization of their electron bands and that they induce unexpected spin transport phenomena. We first show that  $p$ -wave magnetism can coexist with conventional superconductivity regardless of the magnitude of the spin splitting. We then predict that  $p$ -wave magnets induce a charge-to-spin conversion, which can be strongly enhanced by the presence of superconductivity providing a way to probe the coexistence in experiments. Our results open a new avenue for material combinations with a synergetic relation between spintronics and superconductivity.

*Introduction.* – Materials displaying magnetic order is a major topic in condensed matter physics. They have found utility in a range of existing technologies, and continue to attract attention due to their rich quantum physics. A wealth of different magnetic states exist, from collinear ferromagnets to complex spin textures like skyrmions [1, 2].

The spatial texture of a magnetic order heavily influences the properties of electrons in magnetic materials. A prominent example of this is the recently discovered altermagnetism [3–8], where the magnetic sublattices are connected via time-reversal and spatial rotation [9, 10]. This gives rise to a momentum-dependent spin polarization while the material as a whole has no net magnetization or stray field. Such a scenario is of high interest in the field of spintronics [11]. Originating from the exchange interaction, the spin-splitting can be very large in altermagnets compared to the splitting due to spin-orbit interactions.

The spin-dependent bands of a simple model for altermagnets have the same structure in momentum space as the Cooper pair wavefunction in high-temperature superconductors (SC) [12], both exhibiting a  $d$ -wave symmetry. In superfluid He-3 [13], antisymmetric  $p$ -wave Cooper pairs emerge instead. Interestingly, such a superfluid state also has a magnetic equivalent; see Ref. [14] for a recent perspective.

In helimagnetic systems, the localized spin moments form a rotating pattern which causes a  $p$ -wave spin polarization to emerge [15–17] in the itinerant electron bands moving on top of this magnetic background. Such a spin polarization has also been predicted to occur in other systems [18–23]. The precise symmetry requirements for realization of  $p$ -wave spin-polarized bands from magnetic textures, such as  $T\tau$ -symmetry ( $T$  being time-reversal and  $\tau$  translation by a fixed number of lattice sites), were recently established [24, 25] and a minimal effective model was derived [26].

The minimal model shows that a  $p$ -wave magnet ( $pM$ ) exhibits large tunneling magnetoresistance and spin-anisotropic transport [26]; a similar conclusion about the anisotropic transport was later reached in Ref. [27]. Furthermore,  $p$ -wave magnetism affects the longitudinal electron transport in superconducting junctions [28, 29] and provides a possibility

of charge-to-spin conversion via, e.g., second-order spin current [26], transverse spin current in junctions with normal metal (NM) [30], and non-relativistic Edelstein effect [31]; a spin-to-charge conversion in a  $pM$ , i.e., spin-galvanic effect, was recently studied in Ref. [32].

Since the band structure in a  $pM$  has the same structure in momentum space as the Cooper pair wavefunction in superfluid He-3, an intriguing question is to what extent  $pM$  can coexist with superconductivity and if the interplay of magnetism and superconductivity can give rise to new quantum phenomena. In this Letter, we show that the answers to both these questions are in the affirmative.

We demonstrate that unconventional electron spin splitting in  $pM$  is, in fact, perfectly compatible with superconductivity. This holds regardless of the strength of the spin-splitting, suggesting that spontaneous coexistence of these two phases should be possible in a material. We also show that superconductivity plays a surprising role in charge-to-spin conversion: applying an electric voltage to a junction with a  $pM$  generates a transverse spin current that is strongly enhanced by Andreev reflections. This enhanced conversion occurs in a  $pM$ -SC junction and when  $p$ -wave magnetism and superconductivity coexist intrinsically suggesting a way to experimentally probe the coexistence. Our results establish a new arena for material combinations with a synergetic relation between spintronics and superconductivity.

*Proximity-induced superconductivity in  $pM$ .* – The coexistence of  $p$ -wave magnetism and superconductivity depends crucially on whether one considers pairing between normal-state electrons described by  $c, c^\dagger$  or the long-lived quasiparticles described by  $\gamma, \gamma^\dagger$  that are the elementary excitations of the  $pM$  state. The former scenario is relevant for hybrid structures of  $pM$  and SC, which we consider in this section. In this case, superconducting pairing takes place between normal-state electrons in a  $pM$  whereas magnetism is induced on top of the superconducting state via the inverse proximity effect.

To model the  $pM$ , we consider a lattice model with a helical magnetic texture and a mean-field on-site superconductivity

described by the tight-binding Hamiltonian

$$H = -t \sum_{\langle i,j \rangle, \sigma} c_{i,\sigma}^\dagger c_{j,\sigma} - \sum_{i,\sigma,\sigma'} \mathbf{S}_i \cdot c_{i,\sigma}^\dagger \boldsymbol{\sigma}_{\sigma\sigma'} c_{i,\sigma'} - \mu \sum_{i,\sigma} c_{i,\sigma}^\dagger c_{i,\sigma} - \sum_i (\Delta_i c_{i\downarrow}^\dagger c_{i\uparrow}^\dagger + \Delta_i^* c_{i\uparrow} c_{i\downarrow}), \quad (1)$$

where the magnetization  $\mathbf{S}_i$  rotates in a plane perpendicular to the helical ( $x$ ) axis with a period  $\lambda$  and magnitude  $S$ , see the inset in Fig. 1(a) for a schematic of the helimagnetic chain. The superconducting potential  $\Delta_i$  is calculated self-consistently, assuming a constant attractive potential  $U$  in the system. The model is extended to two dimensions (2D) by making  $N_y$  copies of the helical chains stacked in the  $y$ -direction; the number of sites in the  $x$ -direction is  $N_x$ . We apply periodic boundary conditions along the  $y$ -axis and open boundary conditions along the  $x$ -axis. The electron (creation) annihilation operator for an electron with spin projection  $\sigma = \uparrow, \downarrow$  at site  $i$  is denoted by  $c_{i,\sigma}^{(\dagger)}$ . The parameter  $t$  corresponds to hopping between nearest neighbors  $\langle i, j \rangle$  and  $\mu$  is the chemical potential.

The band structure in the bulk of  $pM$  is shown in Fig. 1(a) and demonstrates odd-parity bands with the spin polarization perpendicular to localized spins. To calculate the superconducting critical temperature in this model, we employ the lattice Bogolyubov–de Gennes formalism assuming that the pairing takes place between the normal state electrons, see the SM [33] for details. As we show in Fig. 1(b), the superconducting critical temperature decreases with an increasing period of the magnetic texture of the  $pM$  [34]. This can be understood physically as follows. As the period  $\lambda$  of the magnetic texture increases, the magnetization becomes more homogeneous. The case  $\lambda/a = 2$  ( $a$  is the lattice constant) corresponds to a collinear antiferromagnet, whereas  $\lambda/a \geq 3$  is a helical structure featuring  $p$ -wave spin-polarized bands. The  $p$ -wave symmetry is robust against the presence of spin-orbit coupling (SOC) for even  $\lambda/a$ , but is destroyed by SOC for odd  $\lambda/a$  [24]. When  $\lambda$  is small or comparable to the superconducting coherence length  $\xi$ , the Cooper pairs experience a mostly compensated magnetization. This scenario accommodates a superconducting state coexisting with a spin-splitting that is even larger than the superconducting gap. For very large values of  $\lambda/\xi$ , however, the Cooper pairs experience a magnetic texture resembling a macrospin ferromagnet. Such a ferromagnet is known to destroy superconductivity at the Clogston-Chandrasekhar (CC) limit [35, 36]. Our numerical simulations confirm that the critical spin-splitting field is lowered toward the CC limit as  $\lambda$  increases. Since the coherence length is also affected by  $S$  and  $\lambda$ , there is no sharp boundary between the cases  $\lambda \lesssim \xi$  and  $\lambda \gtrsim \xi$ .

*Coexistence of  $p$ -wave magnetism and superconductivity.*

– To address intrinsic superconductivity and its coexistence with magnetism, we use the following low-energy 2D bulk

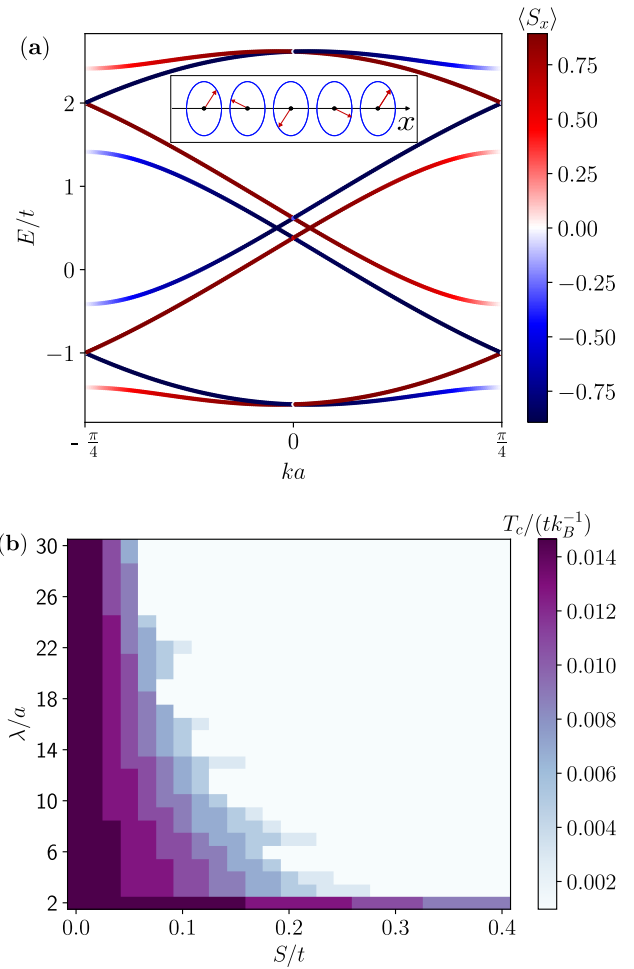


FIG. 1. (a) The band structure for  $\lambda/a = 4$  and  $S = 0.5t$  as a function of the momentum  $k$  in the  $x$ -direction. The energy  $E$  is calculated with respect to the chemical potential. The insert shows the helical magnetization texture. (b) The critical temperature of the superconducting helimagnet as a function of the magnet strength  $S$  and the rotation period  $\lambda$ . In (b), the parameters used are  $\mu = -2.5t$ ,  $N_x = 60$ ,  $N_y = 200$ , and  $U = 1.7t$ .

model [37]:

$$H_{\text{BdG}}(\mathbf{k}) = (\xi_k - \tilde{J}) \tau_z \otimes \rho_0 + \frac{(\mathbf{k} \cdot \boldsymbol{\zeta})}{m} \tau_0 \otimes \rho_z + \frac{\tau_x + i\tau_y}{2} \otimes \hat{\Delta}(\mathbf{k}) + \frac{\tau_x - i\tau_y}{2} \otimes \hat{\Delta}^\dagger(\mathbf{k}), \quad (2)$$

see SM [33] for the derivation. In essence, this is the model presented in the SM of Ref. [26] in the limit of strong intersectoral coupling. The model is also qualitatively similar to that used in Refs. [28–30, 38, 39], which resembles the electron Hamiltonian for the persistent spin helix [18–20]. The Pauli matrices  $\boldsymbol{\tau}$  and  $\boldsymbol{\rho}$  act in the Nambu and band spaces, respectively. Note that due to the presence of the sd coupling, the band basis is not the same as the spin basis; the difference is, however, negligible for a strong intersectoral coupling. To simplify the notations, we introduced  $\xi_k = k^2/(2m) - \mu$ ,  $\tilde{J} = \sqrt{J_{\text{sd}}^2 + t_{\text{inter}}^2}$ ,

and  $\zeta = t_{\text{inter}}\alpha/(2\tilde{J})$ . Here,  $m$  is the effective mass,  $t_{\text{inter}}$  is the inter-sectoral coupling,  $J_{\text{sd}}$  is the sd coupling, and  $\alpha$  is the spin-splitting vector. The order parameter in the band basis is defined as  $\hat{\Delta}(\mathbf{k}) = i\rho_y [\Delta_0(\mathbf{k}) + (\boldsymbol{\rho} \cdot \Delta(\mathbf{k}))]$ , where we separate the amplitude and the angular-dependent parts as  $\Delta(\mathbf{k}) = \phi v(\mathbf{k})$ .

As follows from the  $p$ -wave structure of the energy spectrum, see the lowest two energy bands in Fig. 1(a), a uniform spin-singlet SC order parameter is allowed in the  $s$ -wave channel, and the mixed-spin spin-triplet one exists in the  $p$ -wave channel. The equal-spin spin-triplet pairing has a nonzero center of mass momentum and will be considered elsewhere.

By using the Hamiltonian (2), we derive the gap equation via the function integral approach [33],

$$\phi = g \frac{\nu_0}{2} \int_{-\omega_D}^{\omega_D} d\xi_k \int_0^{2\pi} \frac{d\theta}{2\pi} \sum_j \frac{\partial \epsilon_{j,k}}{\partial \phi^*} \frac{1}{1 + e^{-\epsilon_{j,k}/T}}, \quad (3)$$

where  $g$  is the interaction strength,  $\nu_0 = m/(2\pi)$  is the normal-state DOS,  $\omega_D$  is the Debye frequency that provides a cutoff for the pairing interactions,  $T$  is temperature, and  $\epsilon_{j,k}$  are eigenvalues of  $H_{\text{BdG}}(\mathbf{k})$ . The solution to Eq. (3) minimizes the free energy with respect to the normal state.

We consider superconducting pairing in the  $s$ -wave spin-singlet and  $p$ -wave spin-triplet channels quantified by  $\Delta_0 = \phi$  and  $\Delta_z(\mathbf{k}) = \sqrt{2}\phi \cos(\theta)$ , respectively. By redefining the momentum as  $\mathbf{k} \rightarrow \mathbf{k}_\sigma = \mathbf{k} + \sigma\zeta$  and integrating over the corresponding  $\xi_{k,\sigma}$ , we arrive to the same  $s$ -wave gap and the critical temperature as in the regular BCS superconductors, see, e.g., Ref. [40]. This originates from the structure of the model (2), where the pairing between fermions of opposite spins and at the opposite momenta is always possible and does not depend on the splitting of the bands. The  $p$ -wave mixed-spin spin-triplet pairing is also allowed but is energetically unfavorable compared to the  $s$ -wave gap.

Thus, unlike superconductivity in altermagnets [41–46], it is possible to achieve the coexistence of magnetism and superconductivity for the simplest spin-singlet  $s$ -wave pairing.

*Transport properties.* – The unusual spin-polarized band structure of  $p\text{M}$  and the coexistence of magnetism and superconductivity are directly manifested in transport phenomena. Charge and spin transport in a non-superconducting case [26, 30] and longitudinal transport in junctions with superconductors [28, 29] have very recently been studied. To address the spin transport properties of superconducting junctions, we employ the following model:

$$\begin{aligned} H_{\text{BdG}}(x) = & \left[ \left( k_y^2 - \nabla_x^2 \right) / (2m) - \mu - \tilde{J}(x) \right] \tau_z \otimes \rho_0 \\ & - \Delta(x) \tau_y \otimes \rho_y + U \delta(x) \tau_z \otimes \rho_0 + \frac{\zeta_y(x) k_y}{m} \tau_0 \otimes \rho_z \\ & + \frac{1}{2m} \{ \zeta_x(x), -i\nabla_x \} \tau_0 \otimes \rho_z, \end{aligned} \quad (4)$$

see also Eq. (2) for the bulk Hamiltonian. We assume the spin-singlet  $s$ -wave superconducting gap at  $x > 0$  with  $\Delta(x) = \Delta\Theta(x)$ . The spin-splitting parameter  $\zeta(x)$  and the sd coupling

term  $J_{\text{sd}}(x)$  are nonzero either at  $x < 0$  in the  $p\text{M-SC}$  junction or at  $x > 0$  in the NM-superconducting  $p$ -wave magnet (NM-SC $p\text{M}$ ) one. To model a nonideal interface, we include the barrier potential  $U \delta(x)$ .

In calculating the transport properties of the junctions, we use the standard formalism based on the impinging, scattered, and transmitted waves, see SM [33] for details. We focus on the transport coefficients averaged over the transverse coordinate  $x$ . In this case, the contributions from the interface-localized modes become negligible. The transverse spin conductance is determined by integrating the corresponding spin current over all transverse momenta  $k_y$ :

$$G_{S,j}(V) = -e \int_{-\infty}^{\infty} \frac{dk_y}{(2\pi)^2} \left| \frac{\partial k_x}{\partial \epsilon} \right| I_{S,j}(eV, k_y), \quad (5)$$

where the spin current per  $k_y$  is

$$I_{S,j}(\epsilon, k_y) = \sum_{\sigma=\pm} \text{Re} \{ \Psi_\sigma^\dagger \hat{v}_j \hat{s}_z \Psi_\sigma \} \quad (6)$$

with  $\hat{v}$  being the velocity operator,  $\hat{s}_z$  being the spin operator, and  $\Psi_\sigma$  being the scattering state with the spin projection  $\sigma$ . For the transverse spin current in a  $p$ -wave magnet, we have  $\hat{v}_y \hat{s}_z = t_{\text{inter}} (k_y \tau_0 \otimes \rho_z + \zeta_y \tau_z \otimes \rho_0) / (m\tilde{J})$ . Then, the spin current reads

$$I_{S,y}(\epsilon, k_y) = \frac{t_{\text{inter}}}{m\tilde{J}} \sum_{\sigma=\pm} s k_{y,\sigma} [1 - |a_\sigma(k_y)|^2 + |b_\sigma(k_y)|^2], \quad (7)$$

where  $a_\sigma(k_y)$  and  $b_\sigma(k_y)$  are Andreev and normal reflection amplitudes, respectively, that are found by matching the wave functions and their derivatives [47] at  $x = 0$ . In the NM, one has to replace  $\tilde{J} \rightarrow t_{\text{inter}}$  and  $k_{y,s} \rightarrow k_y$ . Each of the terms in the square brackets contributes only when the corresponding quasiparticles, i.e., retroreflected holes and reflected electrons, are propagating. Impinging electrons are always propagating with the real wavevector  $k_x = -\sigma\zeta_x + \sqrt{2m(\mu + \tilde{J} + \epsilon) - k_{y,\sigma}^2 + |\zeta|^2}$ .

The normalized transverse spin conductance is shown in Fig. 2. It relies on the spin-splitting vector having a nonzero component along the junction. Due to the symmetry of the spin-polarized bands, there is no longitudinal spin current. The superconducting gap strongly affects the spin conductance allowing for the enhanced subgap conductance in an ideal contact, see solid lines in Fig. 2, and a well-pronounced peak at  $|eV| \gtrsim \Delta$  in a tunneling regime, see dashed lines in Fig. 2. The Andreev-enhanced transverse spin conductance is in drastic contrast with the longitudinal spin conductance in ferromagnet-SC junctions [48], where both normal and Andreev reflections reduce the conductance. Whereas efficient charge-to-spin conversion is thus possible by a longitudinal charge current converting into a transverse spin current, superconductivity strongly enhances the charge-to-spin conversion rate in both  $p\text{M-SC}$  and NM-SC $p\text{M}$  junctions. This enhancement occurs in the experimentally relevant regime of low interface transparency, such that the effect does not rely on an idealized, perfect interface.

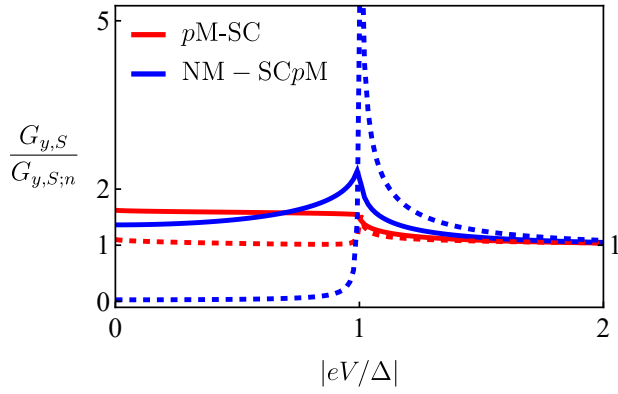


FIG. 2. Transverse spin conductance in the non-superconducting parts of the  $p$ M-SC (red lines) and NM-SC $p$ M (blue lines) junctions for an idea contact (solid lines,  $Z = 0$ ) and in the tunneling limit (dashed lines,  $Z = 10$ ). We normalize by the normal-state transverse spin conductance denoted as  $G_{y,S;n}$  (we set  $|eV|/\Delta = 3$  in  $G_{y,S}$ ) and fixed  $\zeta_x = 0$ ,  $\zeta_y = 0.5 k_F$ , and  $J = 0$ . In addition, we denote  $Z = U\sqrt{2m}/\mu$  and  $k_F = \sqrt{2m\mu}$ .

The physical origin of the Andreev-enhanced spin conductance seen in Fig. 2 is related to the momentum-space structure of the transport coefficients, which, in turn, depends on the overlap of the Fermi surfaces, see Fig. 3. The coefficient  $|a_s(k_y)|^2$  that determines the Andreev reflections requires an overlap between the normal-state Fermi surface in the SC and the Fermi surfaces in the  $p$ M, see the red color in Fig. 3. This means that  $s \sum_{k_y} k_{y,s} |a_s(k_y)|^2 > 0$ . On the other hand, the coefficient for normal reflections  $|b_s(k_y)|^2$  is dominated by the parts of the Fermi surfaces in  $p$ M that have no overlap with that on the SC side, see the blue color in Fig. 3. This results in  $s \sum_{k_y} k_{y,s} |b_s(k_y)|^2 < 0$ . Thus, since the first term in the square brackets in Eq. (7) vanishes after integrating over momenta, both Andreev and normal reflections enhance the transverse spin conductance.

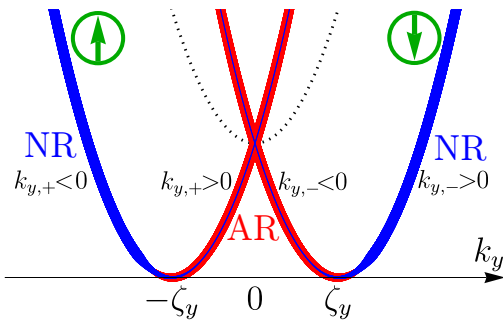


FIG. 3. Schematic depiction of spin-down (right parabola) and spin-up (left parabola) bands on the  $p$ M-side of the  $p$ M-SC junction. The bands are separated by  $2\zeta_y$  along  $k_y$ . The dotted line corresponds to the normal-state Fermi surface on the SC side of the junction. Andreev reflection (AR) and normal reflection (NR) coefficients are shown in red and blue colors, respectively. The former relies on the overlap between the Fermi surfaces on both sides of the junction.

*Concluding remarks.* – We showed that magnetic order in  $p$ -wave magnets coexists with spin-singlet superconductivity. In proximity setups, coexistence quantified by the critical temperature is controlled by the period of the helical magnetic texture in the magnet and the coherence length of the superconductor. The CC limit is exceeded by almost an order of magnitude when the period of the texture  $\lambda$  becomes smaller than the coherence length  $\xi$ , see Fig. 1, and approaches the CC limit at  $\xi \ll \lambda$ . The results for the intrinsic spin-singlet pairing in the effective low-energy model also support the coexistence of superconductivity and magnetism in a bulk  $p$ M.

The interplay of  $p$ -wave spin polarization and superconductivity is manifested in the transport properties of junctions exemplified by the transverse spin current. Contrary to the longitudinal spin conductance in ferromagnet-superconductor junctions,  $p$ -wave magnets allow for transverse spin conductance that is enhanced by Andreev reflections, see Fig. 2. This enhancement is directly related to the structure and spin polarization of the  $p$ -wave spin-polarized bands. A qualitatively similar normalized spin conductance is observed for  $p$ M-SC and NM-SC $p$ M junctions, see Fig. 2, allowing one to identify SC $p$ M in transport measurements.

The proposed coexistence and spin transport could be realized in  $p$ M-candidates CeNiAsO and Mn<sub>3</sub>GaN [25]. Helimagnets with  $p$ -wave polarization such as MnP, FeP, CrAs [49], MnAu<sub>2</sub> [50], MnGe [51], MnSi [52], and  $\alpha$ -EuP<sub>3</sub> [53] should also allow for some of the proposed effects.

To the best of our knowledge, no conclusive experimental observation of coexistent helimagnetic and superconducting order has been reported so far. Our results provide guidance on how the interplay between  $p$ -wave magnetism and superconductivity, including their coexistence, can be probed and suggest a promising platform for investigating the interplay of superconductivity and magnetization thus enriching the field of spintronics.

*Acknowledgments.* – We thank Hendrik Bentmann for pointing out the similarity of the band structure of  $p$ -wave magnets and the persistent spin helix structures and Erik W. Hodt for many useful discussions. This work was supported by the Research Council of Norway through Grant No. 323766 and its Centres of Excellence funding scheme Grant No. 262633 “QuSpin.” Support from Sigma2 - the National Infrastructure for High Performance Computing and Data Storage in Norway, project NN9577K, is acknowledged.

- [1] N. Nagaosa and Y. Tokura, Topological properties and dynamics of magnetic skyrmions, *Nat. Nanotech.* **8**, 899 (2013).
- [2] A. Fert, N. Reyren, and V. Cros, Magnetic skyrmions: Advances in physics and potential applications, *Nat Rev Mater* **2**, 17031 (2017).
- [3] Y. Noda, K. Ohno, and S. Nakamura, Momentum-dependent band spin splitting in semiconducting MnO<sub>2</sub>: a density functional calculation, *Phys. Chem. Chem. Phys.* **18**, 13294 (2016).
- [4] K.-H. Ahn, A. Hariki, K.-W. Lee, and J. Kuneš, Antiferromag-

- netism in RuO<sub>2</sub> as *d*-wave Pomeranchuk instability, *Phys. Rev. B* **99**, 184432 (2019).
- [5] S. Hayami, Y. Yanagi, and H. Kusunose, Momentum-Dependent Spin Splitting by Collinear Antiferromagnetic Ordering, *J. Phys. Soc. Jpn.* **88**, 123702 (2019).
- [6] L.-D. Yuan, Z. Wang, J.-W. Luo, E. I. Rashba, and A. Zunger, Giant momentum-dependent spin splitting in centrosymmetric low-*Z* antiferromagnets, *Phys. Rev. B* **102**, 014422 (2020).
- [7] L. Šmejkal, R. González-Hernández, T. Jungwirth, and J. Sinova, Crystal time-reversal symmetry breaking and spontaneous Hall effect in collinear antiferromagnets, *Science advances* **6**, eaaz8809 (2020).
- [8] H.-Y. Ma, M. Hu, N. Li, J. Liu, W. Yao, J.-F. Jia, and J. Liu, Multifunctional antiferromagnetic materials with giant piezomagnetism and noncollinear spin current, *Nat Commun* **12**, 2846 (2021), arXiv:2104.00561 [cond-mat.mtrl-sci].
- [9] L. Šmejkal, J. Sinova, and T. Jungwirth, Emerging Research Landscape of Altermagnetism, *Phys. Rev. X* **12**, 040501 (2022).
- [10] L. Šmejkal, J. Sinova, and T. Jungwirth, Beyond Conventional Ferromagnetism and Antiferromagnetism: A Phase with Nonrelativistic Spin and Crystal Rotation Symmetry, *Phys. Rev. X* **12**, 031042 (2022).
- [11] A. Hirohata, K. Yamada, Y. Nakatani, I.-L. Prejbeanu, B. Diény, P. Pirro, and B. Hillebrands, Review on spintronics: Principles and device applications, *Journal of Magnetism and Magnetic Materials* **509**, 166711 (2020).
- [12] B. Keimer, S. A. Kivelson, M. R. Norman, S. Uchida, and J. Zaanen, From quantum matter to high-temperature superconductivity in copper oxides, *Nature* **518**, 179 (2015), arXiv:1409.4673 [cond-mat.supr-con].
- [13] A. J. Leggett, A theoretical description of the new phases of liquid <sup>3</sup>He, *Rev. Mod. Phys.* **47**, 331 (1975).
- [14] T. Jungwirth, R. M. Fernandes, E. Fradkin, A. H. MacDonald, J. Sinova, and L. Šmejkal, From superfluid <sup>3</sup>He to altermagnets (2024), arXiv:2411.00717 [cond-mat].
- [15] I. Martin and A. F. Morpurgo, Majorana fermions in superconducting helical magnets, *Phys. Rev. B* **85**, 144505 (2012).
- [16] G. Chen, M. Khosravian, J. L. Lado, and A. Ramires, Designing spin-textured flat bands in twisted graphene multilayers via helimagnet encapsulation, *2D Mater.* **9**, 024002 (2022).
- [17] A. H. Mayo, D.-A. Deaconu, H. Masuda, Y. Nii, H. Takahashi, R. V. Belosludov, S. Ishiwata, M. S. Bahramy, and Y. Onose, Band-asymmetry-driven nonreciprocal electronic transport in a helimagnetic semimetal  $\alpha$ -EuP<sub>3</sub> (2024), arxiv:2404.13856 [cond-mat].
- [18] J. Schliemann, J. C. Egues, and D. Loss, Nonballistic Spin-Field-Effect Transistor, *Phys. Rev. Lett.* **90**, 146801 (2003), arXiv:cond-mat/0211603.
- [19] B. A. Bernevig, J. Orenstein, and S.-C. Zhang, Exact SU(2) Symmetry and Persistent Spin Helix in a Spin-Orbit Coupled System, *Phys. Rev. Lett.* **97**, 236601 (2006), arXiv:cond-mat/0606196.
- [20] J. Schliemann, Colloquium: Persistent spin textures in semiconductor nanostructures, *Rev. Mod. Phys.* **89**, 011001 (2017), arXiv:1604.02026 [cond-mat.mes-hall].
- [21] S. Hayami, Y. Yanagi, and H. Kusunose, Spontaneous Antisymmetric Spin Splitting in Noncollinear Antiferromagnets without Spin-Orbit Coupling, *Phys. Rev. B* **101**, 220403(R) (2020), arXiv:2001.05630 [cond-mat].
- [22] S. Hayami, Y. Yanagi, and H. Kusunose, Bottom-up design of spin-split and reshaped electronic band structures in spin-orbit-coupling free antiferromagnets: Procedure on the basis of augmented multipoles, *Phys. Rev. B* **102**, 144441 (2020), arXiv:2008.10815 [cond-mat].
- [23] S. Hayami, Mechanism of antisymmetric spin polarization in centrosymmetric multiple-*Q* magnets based on bilinear and biquadratic spin cross products, *Phys. Rev. B* **105**, 024413 (2022), arXiv:2201.01354 [cond-mat].
- [24] Y. B. Kudasov, Topological band structure due to modified kramers degeneracy for electrons in a helical magnetic field, *Phys. Rev. B* **109**, L140402 (2024).
- [25] A. B. Hellenes, T. Jungwirth, J. Sinova, and L. Šmejkal, Exchange spin-orbit coupling and unconventional p-wave magnetism (2023), arXiv:2309.01607v2.
- [26] B. Brekke, P. Sukhachov, H. G. Giil, A. Brataas, and J. Linder, Minimal Models and Transport Properties of Unconventional p-Wave Magnets, *Phys. Rev. Lett.* **133**, 236703 (2024).
- [27] A. B. Hellenes, T. Jungwirth, J. Sinova, and L. Šmejkal, Exchange spin-orbit coupling and unconventional p-wave magnetism (2023), arXiv:2309.01607v3.
- [28] K. Maeda, B. Lu, K. Yada, and Y. Tanaka, Theory of Tunneling Spectroscopy in Unconventional *p*-Wave Magnet-Superconductor Hybrid Structures, *J. Phys. Soc. Jpn.* **93**, 114703 (2024), arXiv:2403.17482.
- [29] Y. Fukaya, K. Maeda, K. Yada, J. Cayao, Y. Tanaka, and B. Lu, Fate of the josephson effect and odd-frequency pairing in superconducting junctions with unconventional magnets (2024), arXiv:2411.02679 [cond-mat.supr-con].
- [30] M. Salehi and A. A. Hedayati, Transverse spin current at the normal/p-wave altermagnet junctions (2024), arXiv:2408.10413 [cond-mat.mes-hall].
- [31] A. Chakraborty, A. B. Hellenes, R. Jaeschke-Ubiergo, T. Jungwirth, L. Šmejkal, and J. Sinova, Highly Efficient Non-relativistic Edelstein effect in p-wave magnets (2024), arXiv:2411.16378 [cond-mat].
- [32] T. Kikkeler, I. Tokatly, and F. S. Bergeret, Quantum transport theory for unconventional magnets; interplay of altermagnetism and p-wave magnetism with superconductivity (2024), arXiv:2412.10236 [cond-mat].
- [33] See Supplemental Material for the details of the lattice model, functional integral approach, and transport calculations.
- [34] T. Champel and M. Eschrig, Effect of an inhomogeneous exchange field on the proximity effect in disordered superconductor-ferromagnet hybrid structures, *Phys. Rev. B* **72**, 054523 (2005).
- [35] A. M. Clogston, Upper Limit for the Critical Field in Hard Superconductors, *Phys. Rev. Lett.* **9**, 266 (1962).
- [36] B. S. Chandrasekhar, A Note on the Maximum Critical Field of High-Field Superconductors, *Appl. Phys. Letters* **1**, 1 (1962).
- [37] In writing Eq. (2), we used the basis  $\{c_{\uparrow}, c_{\downarrow}, c_{\uparrow}^{\dagger}, c_{\downarrow}^{\dagger}\}$ . For this effective model, original  $(c_{\sigma}, c_{\sigma}^{\dagger})$  and diagonal  $(\gamma, \gamma^{\dagger})$  bases coincide.
- [38] M. Ezawa, Purely electrical detection of the Néel vector of *p*-wave magnets based on linear and nonlinear conductivities (2024), arXiv:2410.21854 [cond-mat].
- [39] M. Ezawa, Third-order and fifth-order nonlinear spin-current generation in *sg*-wave and *si*-wave altermagnets and perfect spin-current diode based on *sf*-wave magnets (2024), arXiv:2411.16036 [cond-mat].
- [40] K. Fossheim and A. Sudbø, *Superconductivity: Physics and Applications* (Wiley, Chichester, West Sussex, England ; Hoboken, NJ, 2004).
- [41] S. Sumita, M. Naka, and H. Seo, Fulde-Ferrell-Larkin-Ovchinnikov state induced by antiferromagnetic order in  $\kappa$ -type organic conductors, *Phys. Rev. Research* **5**, 043171 (2023), arXiv:2308.14227 [cond-mat.supr-con].
- [42] D. Chakraborty and A. M. Black-Schaffer, Zero-field finite-momentum and field-induced superconductivity in altermagnets, *Phys. Rev. B* **110**, L060508 (2024).

- [43] G. Sim and J. Knolle, [Pair Density Waves and Supercurrent Diode Effect in Altermagnets](#) (2024), [arXiv:2407.01513 \[cond-mat\]](#).
- [44] S. Hong, M. J. Park, and K.-M. Kim, Unconventional p-wave and finite-momentum superconductivity induced by altermagnetism through the formation of Bogoliubov Fermi surface (2024), [arXiv:2407.02059 \[cond-mat\]](#).
- [45] A. Bose, S. Vadnais, and A. Paramekanti, [Altermagnetism and superconductivity in a multiorbital t-J model](#) (2024), [arXiv:2403.17050](#).
- [46] D. Chakraborty and A. M. Black-Schaffer, [Constraints on superconducting pairing in altermagnets](#) (2024), [arXiv:2408.03999 \[cond-mat\]](#).
- [47] In matching the derivatives, one needs to take into account the coordinate-dependence of  $\zeta_x(x)$ .
- [48] S. Kashiwaya, Y. Tanaka, N. Yoshida, and M. R. Beasley, Spin current in ferromagnet-insulator-superconductor junctions, *Phys. Rev. B* **60**, 3572 (1999).
- [49] A. Kallel, H. Boller, and E. Bertaut, Helimagnetism in MnP-type compounds: MnP, FeP, CrAs and  $\text{CrAs}_{1-x}\text{Sb}_x$  mixed crystals, *Journal of Physics and Chemistry of Solids* **35**, 1139 (1974).
- [50] A. Herpin and P. Meriel, Étude de l'antiferromagnétisme hélicoïdal de  $\text{MnAu}_2$  par diffraction de neutrons, *J. Phys. Radium* **22**, 337 (1961).
- [51] N. Kanazawa, Y. Onose, T. Arima, D. Okuyama, K. Ohoyama, S. Wakimoto, K. Kakurai, S. Ishiwata, and Y. Tokura, Large Topological Hall Effect in a Short-Period Helimagnet MnGe, *Phys. Rev. Lett.* **106**, 156603 (2011).
- [52] Y. Ishikawa, K. Tajima, D. Bloch, and M. Roth, Helical spin structure in manganese silicide MnSi, *Solid State Communications* **19**, 525 (1976).
- [53] A. H. Mayo, H. Takahashi, M. S. Bahramy, A. Nomoto, H. Sakai, and S. Ishiwata, Magnetic Generation and Switching of Topological Quantum Phases in a Trivial Semimetal  $\alpha$ -EuP<sub>3</sub>, *Phys. Rev. X* **12**, 011033 (2022), [arXiv:2103.13966 \[cond-mat.str-el\]](#).